2018

Numerical Simulation of Fault Impacts for Commercial Walk-in Freezers

Alireza Behfar
University of Nebraska - Lincoln, abehfar@unomaha.edu

David P. Yuill
University of Nebraska-Lincoln, dyuill@unl.edu

2018

Numerical Simulation of Fault Impacts for Commercial Walk-in Freezers

Alireza Behfar
University of Nebraska - Lincoln, United States of America, abehfar@unomaha.edu

David P. Yuill
University of Nebraska-Lincoln, dyuill@unl.edu

Numerical Simulation of Fault Impacts for Commercial Walk-in Freezers

Alireza BEHFAR*, David YUILL

University of Nebraska - Lincoln, Department of Architectural Engineering and Construction, Omaha, Nebraska, USA
abehfar@unomaha.edu

* Corresponding Author

ABSTRACT

Refrigeration systems can undergo many faults that could negatively affect their operation and performance. This paper describes a modeling process to simulate the fault impacts on the operation of a commercial walk-in freezer using semi-empirical models. These models often require less modeling effort than full forward models and could be used in scenarios where detailed information is missing, such as in field-measured systems. An important characteristic of a typical walk-in refrigeration system is the existence of a liquid-line receiver after the condenser, which significantly changes the behavior of the cycle, in comparison to a receiver-less system. Component models described in this paper consist of: a compressor, two heat exchangers, pipelines, receiver, and thermostatic expansion valve. The semi-empirical component models are partially based on physics, and partially based on some empirical coefficients. They are able to predict several dependent variables, including mass flow rates, heat transfer rates, power consumption, and pressures. In this paper, the individual component models are presented and trained with a limited set of faulted and fault-free experimental data. The faults are: heat exchanger fouling, liquid-line restriction, and compressor valve leakage. The results show that models for major components, such as compressor and heat exchangers, give good predictions for some of the most important performance indices. Modeling challenges and future research are outlined.

1. INTRODUCTION

Many common faults, such as heat exchanger fouling or iced-up evaporator, compressor problems, liquid-line restriction, and improper charge levels, can occur in commercial refrigeration systems (Behfar et al. 2017). A fault-enabled model that can consider several important system faults at different severity levels can benefit the refrigeration industry in various ways. It can be used as part of a model predictive control (MPC) for optimal performance (Schalbart et al. 2015; Yin and Li 2016). It can also be used as part of a model-based fault detection and diagnostic (FDD) method or a fault-tolerant control method in which, instead of fixing a fault, the system's controlled variables are changed to compensate for the fault's effects (Izadi-Zamanabadi et al. 2012). Fault-enabled models are also useful to analyze the design and operational characteristics of a component or system for which it is very difficult to do with experiment (ASHRAE 2015). In general, modeling approaches can be broadly categorized into three groups: forward (knowledge-based), semi-empirical (gray-box), and empirical (black-box) models (Oussar and Dreyfus 2001). Semi-empirical models gain an advantage over other modeling approaches as they partially represent physical characteristics of a component and have the training flexibility of an empirical model and, therefore, allow for the creation of a detailed model with a reasonable effort (Oussar and Dreyfus 2001). Cheung and Braun (2013) created several detailed semi-empirical fault-enabled computer models for air conditioning systems consisting of split and rooftop units. They developed individual component models based on the available literature and identified model parameters with the use of a limited set of experimental test data.

Although the fundamental principles of refrigeration are the same, there are major differences between the vapor compression cycle used in the commercial refrigeration systems, such as supermarkets and walk-in coolers and freezers, and those used in the air conditioning systems (Wirz 2009). Differences can both be in operating conditions and/or existing components. Commercial freezers, for example, have a much less evaporating temperature than air conditioning systems. Also, as air conditioning systems, such as rooftop units, usually do not contain a liquid line

refrigerant receiver, they are critically charged. While receivers store the excessive charge in the system, they change the thermodynamic behavior of the system in comparison to one without a receiver (Wichman and Braun 2009). In a system without the receiver, the excess charge backs up in the condenser and increases the subcooling. Neither of the eight systems tested in Cheung and Braun (2013) was a commercial refrigeration system nor contained a liquid-line receiver. The current paper investigates the development and identification of a detailed computer model of a commercial refrigeration system with a liquid-line receiver at the condenser outlet. Individual sub-models for major components, such as a compressor, condenser, evaporator, expansion valve, refrigerant pipeline, and charge inventory, are created and trained with the use of a limited set of experimental data from a commercial walk-in freezer. Core equations are presented and explained, and the prediction results of some of the important performance indices are shown and analyzed. A schematic diagram of a typical commercial walk-in freezer system is shown in Figure 1.

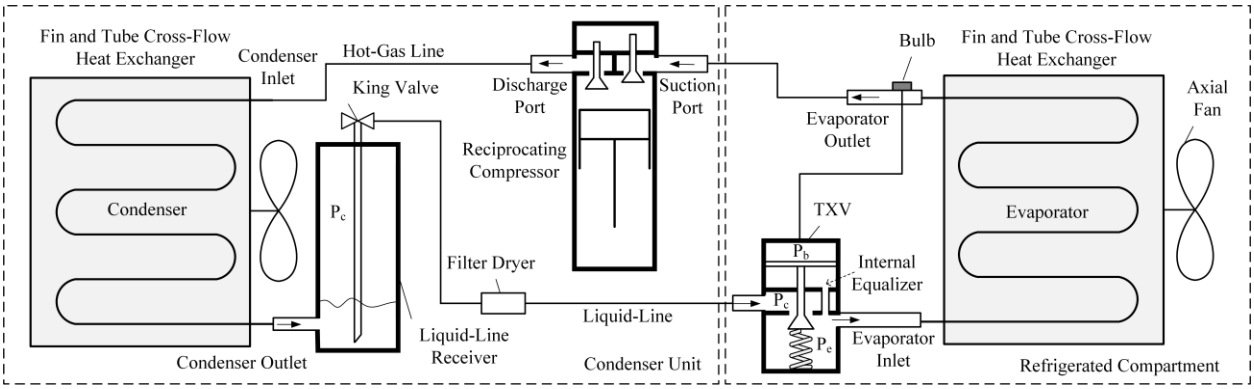

Figure 1: Schematic diagram of a walk-in refrigeration system

2. METHODOLOGY

The modeling approach used in this research includes the creation and identification of several component models based on the available literature, with the use of a limited set of faulted and fault-free experimental datasets. As the experimental data are used to find some unknowns, such a modeling approach makes the process less dependent on detailed prior knowledge of the components' physical characteristics. Although this advantage exists for semi-empirical and empirical models, the emphasis will be on the use of semi-empirical models. Such component functions mainly consist of regression parameters and input variables. Input variables include the direct steady-state temperature and pressure measurements from air or refrigerant sides of a system. The output of the function is a predicted variable, such as heat transfer, mass flow rate, power consumption, and pressure drop, that will be compared with a calculated or a measured value in training and validation processes.

$$Y = function(C_1, C_2, \dots, C_m, var_1, var_2, \dots, var_n) \tag{1}$$

In equation (1), *Y* is the function output, *C* is the regression coefficient, and *var* is the input variable. Other parameters, such as normalization parameters, may also be used. In order to find a set of regression coefficient values, *C*, that provide the best output, the value of the objective function needs to be minimized. That is simply in the form of a difference between the predicted and the measured value of the output (Equation (2)).

$$\varepsilon = \sum_i^z \left(\frac{Y_{predicted,i} - Y_{measured,i}}{Y_{measured,i}} \right)^2 \tag{2}$$

In this research work, available optimization functions (Sequential Quadratic Programming and Interior-Point algorithms) in a mathematical software (MATLAB) are used to minimize objective functions and to find the regression parameters[1]. A thermodynamic calculation software (CoolProp) was incorporated into model codes for refrigerant property calculations. Weighting factors were applied to the optimization functions as described in Cheung and Braun (2013) to avoid over-emphasizing data points with certain similar measurement values.

[1] Many of the modeling computer codes developed in Cheung (2014) are used in this research.

2.1 System and Data Descriptions

The system in this paper is a packaged commercial walk-in freezer with an air-cooled condenser and evaporator, a single compressor, a TXV, a liquid-line receiver, a filter drier after the receiver, and R404A as the refrigerant (Figure 1). Wichmann and Braun (2009) experimentally simulated five different faults on this system, at the 24°C ambient temperature, consisting of the compressor valve leakage, condenser and evaporator improper air flow rates, undercharge, and liquid line restriction. They measured steady-state data consisting of the refrigerant side temperatures and pressures, refrigerant mass flow rate, compressor power consumption, air side temperatures across heat exchangers, and total system charge. More information about the system and fault severity levels can be found in Wichmann and Braun (2009). In the current paper, the dataset is divided into training and validation sets. Several faulted test data were randomly excluded from the dataset for validation purposes, which also includes several simultaneous faults.

The experimental refrigerant mass flow rate measurements for the two most severe undercharge faults and a simultaneous fault test including a severe undercharge fault were invalid. Because the liquid-line tends to have little or no subcooling in such systems, the refrigerant is susceptible to a phase change from a saturated liquid to a two-phase condition. That, in turn, causes a two-phase refrigerant to enter the mass flow meter, increasing the risk of invalid measurements. In order to avoid discarding the experimental data of those tests altogether, the refrigerant mass flow rate of those cases was estimated with the use of the adjusted compressor map from the compressor manufacturer based on the suction line superheat (Dabiri and Rice 1981).

2.2 Compressor

The purpose of a compressor model is to predict the refrigerant mass flow rate, power consumption, and enthalpy rise across the compressor. The common 10-coefficient compressor map equation that is typically used by manufacturers is used to model the compressor mass flow rate and power consumption (Standard AHRI 2015). It uses evaporating, T_e, and condensing, T_c, temperatures and 10 coefficients, C, to predict the mass flow rate and power consumption.

$$\dot{m}_{r,comp} = C_1 + C_2T_e + C_3T_e^2 + C_4T_e^3 + C_5T_c + C_6T_c^2 + C_7T_c^3 + C_8T_eT_c + C_9T_eT_c^2 + C_{10}T_e^2T_c \quad (3)$$

The power consumption can be calculated with the same form as equation (3). The heat loss out of the compressor and the outlet refrigerant enthalpy can be calculated based on the available sensor data, such as the inlet and outlet refrigerant temperatures and ambient temperature and based on the first law of thermodynamics (Cheung and Braun 2013).

$$f_{comp} = 1 + C_1\dot{m}_r + \frac{C_2}{T_{r,comp,in}} + \frac{C_3}{T_{r,comp,out}(P_{sat})} \quad (4)$$

$$\dot{Q}_{HL} = (C_4 + C_5(T_{r,comp,in} - T_{amb}) + C_6(T_{r,comp,out} - T_{amb}))/f_{comp} \quad (5)$$

$$h_{r,comp,out} = h_{r,comp,in} + \frac{\dot{W}_{comp} - \dot{Q}_{HL}}{\dot{m}_r} \quad (6)$$

In equations (4) to (6), $\dot{Q}$ is the heat transfer, $\dot{W}$ is the power, h is the enthalpy, T is the temperature, $\dot{m}$ is the refrigerant mass flow rate, and C is the regression parameter.

2.3 Condenser

As the refrigerant passes through a condenser, it normally experiences three different phases: superheated, two-phase, and subcooled. Crossflow air-cooled fin-and-tube condensers are widely used in commercial refrigeration systems. The purpose of a detailed heat exchanger model is to predict the heat transfer rates across each section of the heat exchangers, pressure drop, and absolute amount of the charge as well as the thermodynamic state of the refrigerant at various points in the condenser. The heat exchanger model proposed in Bell (2010) is the most updated heat exchanger model in the literature that uses a moving boundary method of heat transfer calculations. The model needs the heat transfer conductance, UA, to solve the total heat transfer rate in each boundary via the Number of Transfer Units (NTU) method. To calculate the conductance in a forward modeling approach, detailed geometrical knowledge of a heat exchangers including the number of fins, fin spacing, and air-side and refrigerant-side surface areas are needed (Bergman et al. 2011) that are typically unavailable to a modeler. Cheung and Braun (2013) modified the model by Bell (2010) and made it less dependent on geometrical parameters, hence creating a semi-empirical model:

$$UA_{a,cond} = U_{a,cond,reg}\left(\frac{\dot{m}_a}{\dot{m}_{a,cond,rated}}\right)^{n_{a,cond,reg}} A_{r,cond,rated} \quad (7)$$

Equation (7) relates the air side conductance, $UA_{a,cond}$, to the air flow rate across the condenser. On the refrigerant side, the heat transfer conductance of the two-phase section is assumed to be directly proportional to the refrigerant mass flow rate as shown in equation (8).

$$UA_{r,cond,tp} = U_{r,cond,tp,reg}\left(\frac{\dot{m}_r}{\dot{m}_{r,rated}}\right) A_{r,cond,rated} \quad (8)$$

Single-phase sections are modeled with the use of Dittus-Boelter equation (Incropera et al. 2007) for turbulent flow in a smooth circular tube (Equation (9)).

$$UA_{r,cond,1\phi} = \frac{U_{r,cond,1\phi,reg}}{K_{r,cond,1\phi}} \left(\frac{c_{r,1\phi}\mu_{r,1\phi}}{K_{r,1\phi}}\right)^{0.4} \left(\frac{\dot{m}_r}{\mu_{r,1\phi}}\right)^{0.8} A_{r,cond,rated} \quad (9)$$

For heat transfer model, there are five regression parameters in equations (7) to (9): $U_{a,cond,reg}$, $n_{a,cond,reg}$, $U_{r,cond,tp,reg}$, and two coefficients of $U_{r,cond,1\phi,reg}$ for single phase cases of superheated and subcooled sections. The output of the condenser heat transfer model includes thermodynamic states at the outlet of the condenser as well as the area ratios, ω, associated with each moving boundary. The pressure drop is modeled by considering the frictional and acceleration losses in the condenser (Cheung and Braun 2013):

$$\begin{aligned}\Delta P_{r,evap} = {} & \omega_{r,cond,sh} C_{r,cond,\Delta P,sh} \left(\frac{\dot{m}_r^2}{\rho_{r,cond,v}}\right)\left(\frac{\rho_{r,cond,rated}}{\dot{m}_{r,rated}^2}\right) \\ & + \omega_{r,cond,\mathrm{tp}} C_{r,\mathrm{cond},\Delta P,\mathrm{tp},1} \left(\frac{\dot{m}_r^2}{\rho_{r,cond,\mathrm{tp}}}\right)\left(\frac{\rho_{r,cond,\mathrm{tp},rated}}{\dot{m}_{r,rated}^2}\right)\left(\frac{\mu_{\mathrm{r,cond,in}}}{\mu_{\mathrm{r,cond,v,rated}}}\right)^{\mathrm{C_{r,cond,\Delta P,tp,2}}} \\ & + \omega_{r,cond,sc} C_{r,cond,\Delta P,sc} \left(\frac{\dot{m}_r^2}{\rho_{r,cond,sc}}\right)\left(\frac{\rho_{r,cond,sc,rated}}{\dot{m}_{r,rated}^2}\right) \\ & + C_{r,cond,\Delta \mathrm{P,acc}} \left(\frac{\dot{\mathrm{m}}_r^2}{\dot{\mathrm{m}}_{r,rated}^2}\right) \rho_{r,cond,rated} \left(\frac{1}{\rho_{r,cond,out}} - \frac{1}{\rho_{r,cond,in}}\right)\end{aligned} \quad (10)$$

In equation (10), $C_{r,cond,\Delta P,sh}$, $C_{r,cond,\Delta P,\mathrm{tp},1}$, $\mathrm{C_{r,cond,\Delta P,tp,2}}$, and $C_{r,cond,\Delta P,sc}$ are regression parameters.

2.4 Receiver

A receiver acts as a buffer zone for the system as it operates under various conditions or when the system is low in charge. The liquid level inside the receiver can fluctuate depending on the operating condition, and it is usually designed to hold about 90% of the system charge (Parker 2016). The heat transfer out of the receiver is usually negligible in comparison to the amount of the heat transfer in the condenser. However, the charge inside the receiver should be modeled as part of a refrigeration cycle model. In recent years, there have been several studies on liquid line receivers in HVAC&R as well as the automotive industry. The receiver has been modeled (Assawamartbunlue and Brandemuehl 2000, 2006; Rajapaksha and Suen 2004; Chen and Deng 2006; Rasmussen and Alleyne 2006; Techarungpaisan et al. 2007; Llopis et al. 2008; Wei et al. 2008), and was experimentally tested (Parrino et al. 1999; Finlayson and Dickson 2004; Strupp et al. 2010) in several studies to calculate or obtain parameters, such as heat transfer rate, mass flow rate, and absolute amount of mass in the receiver. Approaches for the refrigerant mass quantity calculation in the literature can be grouped into two categories. One is the dynamic and time-dependent models that need time-series data at certain time intervals, in which multiple equations based on mass and energy conversation equations should be solved simultaneously. The other is to take the volume of heat exchangers and connecting pipelines as known data and to calculate the amount of the charge in the receiver by subtracting the amount of charge in other components from total system charge (Equation 11).

$$M_{receiver} = M_{system} - (M_{cond} + M_{evap} + M_{pipeline}) \quad (11)$$

In this research, to model the charge in the cycle model, assuming that only the excess charge is stored in the receiver, system closure equation (11) and the undercharge fault tests are deployed to obtain a relationship between the total system charge and the charge in the receiver.

2.5 TXV

A thermostatic expansion valve (TXV) is an actuated valve that is intended to maintain a temperature-based setpoint, to protect the compressor from liquid slugging or flooding, by controlling the refrigerant to be superheated at the compressor inlet (Wirz 2009). A detailed TXV model is necessary for modeling the effect of faults in a fault-enabled cycle model.

Several semi-empirical TXV models exist in the literature that are based on the general orifice equation of valve (Cheung and Braun 2013; Eames et al. 2014; Kim and Braun 2016; Li and Braun 2008). In this research, the model that was developed by Kim and Braun (2016) is used:

$$\dot{m}_{max} = C_1\sqrt{2.\rho(P_c - P_e.Z)} \tag{12}$$

$$Z = C_2.\left(\frac{SC+2}{T_{cri}}\right)^{C_3} + C_4.\left(\frac{P_{cri}-P_e}{P_{cri}}\right) + C_5 \tag{13}$$

$$\dot{m}_{TXV} = (C_6 + C_7(P_b - P_e)/\Delta p_{rated} + C_8.((P_b - P_e)/\Delta p_{rated})^2).\dot{m}_{max} \tag{14}$$

for cases where $C_9 < (P_b - P_e) < C_{10}$ (when the valve is modulating).

$$\dot{m} = (C_6 + C_7C_{10}/\Delta p_{rated} + C_8(\frac{C_{10}}{\Delta P_{rated}})^2)\sqrt{\rho(P_c - P_e)} \tag{15}$$

for cases where $(P_b - P_e) > C_{10}$ (when the valve is at the maximum opening).

$$\dot{m} = (C_6 + C_7C_9/\Delta P_{rated} + C_8(C_9/\Delta P_{rated})^2)\sqrt{\rho(P_c - P_e)} \tag{16}$$

for cases where $(P_b - P_e) < C_9$ (when the valve is at the minimum opening).

In Equations (12) to (16), C is a regression coefficient, P is pressure, SC is subcooling at the inlet of the valve, and ρ is the density of refrigerant at the valve inlet.

2.6 Evaporator

As the refrigerant enters the evaporator, that passes a two-phase section after which it continues to absorb the heat of surroundings, and exits as a superheated gas at the evaporator outlet. The evaporator model including equations for calculating the air-side and refrigerant-side conductance resemble those of the condenser with additional wet-coil considerations due to the water condensations on fin and tube surfaces and the associated latent load. As in this research there was no condensation on the coil, the air dew point temperature was set to a very low value (e.g. -40°C) to simulate a dry coil. A complete description of the heat exchanger models including the calculation of the void fraction model is explained in Cheung (2014).

2.7 Pipeline

All pipelines in a typical walk-in unit can be grouped into three sections: liquid-line, suction, and hot gas pipes. Liquid-line and hot gas pipes reject the heat to surroundings while the suction line absorbs the heat of the ambient. Pipelines in such systems experience some air movements, in particular, where they are in the vicinity of the condenser fan flow path. Theoretically, the heat transfer can best be described with the use of a mixed convective heat transfer coefficient, which consists of the Grashoff and Reynolds numbers. While the Grashoff number can be calculated by air side and tube surface temperatures, the Reynolds number requires a knowledge of the airflow speed over pipes. As an appropriate representative air speed on pipes is not available in this research, the heat transfer is modeled by assuming natural convection on a horizontal cylinder in Equation (17) and by taking into account the inner and outer pipe heat transfer coefficients (Cheung and Braun 2013):

$$\dot{m}_r\left(h_{r,pipeline,out} - h_{r,pipeline,in}\right) = \left(\frac{1}{C_1}\left(\frac{T_{amb}}{T_{r,pipeline,in}} - T_{amb}\right)^{C_2} + \frac{1}{C_3\left(\frac{\dot{m}_{r,pipeline,rated}}{\dot{m}_r}\right)^{C_4}}\right)^{-1} * \left(T_{r,pipeline,in} - T_{amb}\right)/\Delta T_{r,pipeline,rated}\dot{m}_{r,pipeline,rated}\Delta h_{r,pipeline,rated} \quad (17)$$

3. RESULTS

In this section, the training and validation results of models for some of the most important performance parameters are presented with the use of parity and residual plots and further analyses of the results are discussed, where necessary. The performance parameters are refrigerant mass flow rate, heat transfer rate in a heat exchanger, and the compressor power consumption.

Figures 2 and 3 show the training and validation performances of the compressor mass flow rate model. In order to avoid extrapolation, the training data set includes the most severe tested fault from each fault category. Both training and validation performances are generally good.

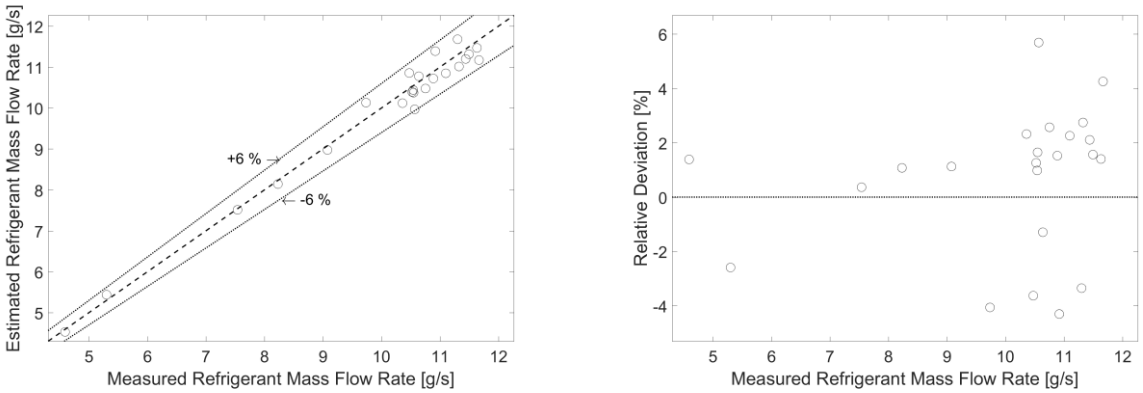

Figure 2: Parity plot (left) and residual plot (right) of compressor training set mass flow rate measured vs. predicted values

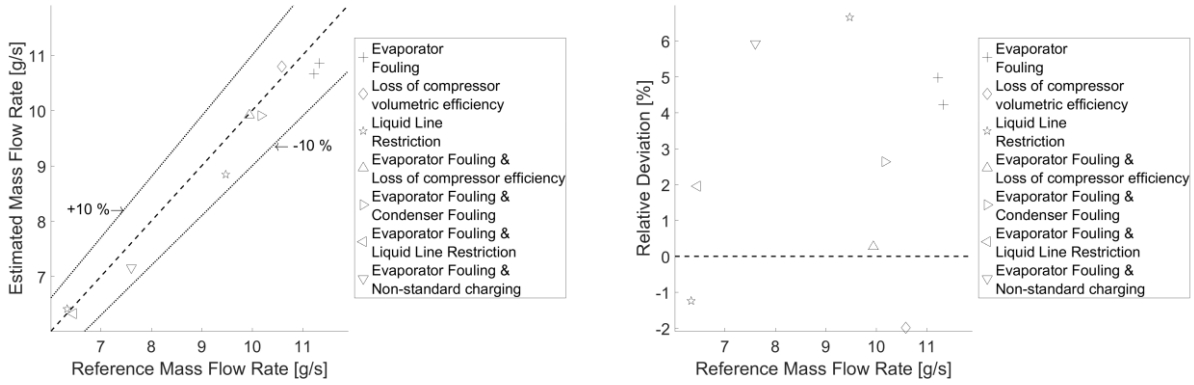

Figure 3: Parity plot (left) and residual plot (right) of compressor validation set mass flow rate measured vs. predicted values

Figures 4 and 5 show the training and validation results of the evaporator heat transfer model. The measured heat transfer rates range from about 600 to more than 1300 W, and predictions closely fit for both training and validation

performance. Although the evaporator model is capable of simulating latent load due to water condensation, the dataset in this research was collected under conditions that caused a dry evaporator coil.

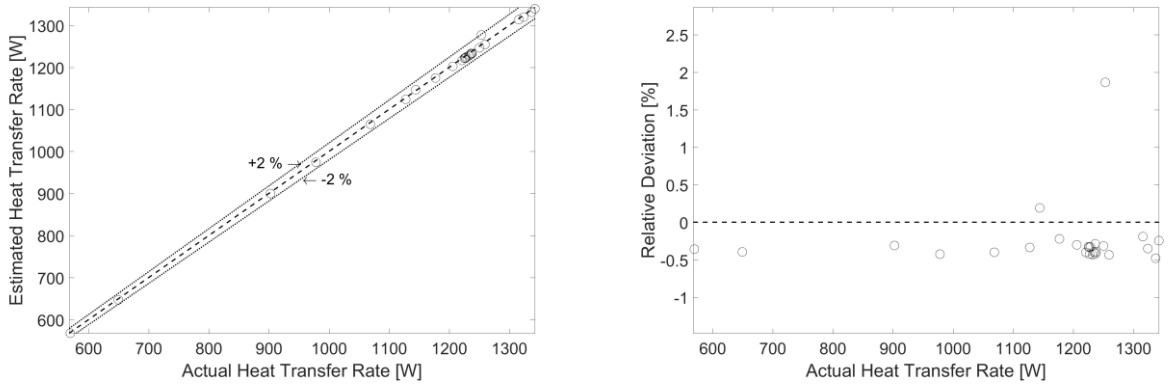

Figure 4: Parity plot (left) and residual plot (right) of evaporator training set heat transfer rate actual vs. predicted values

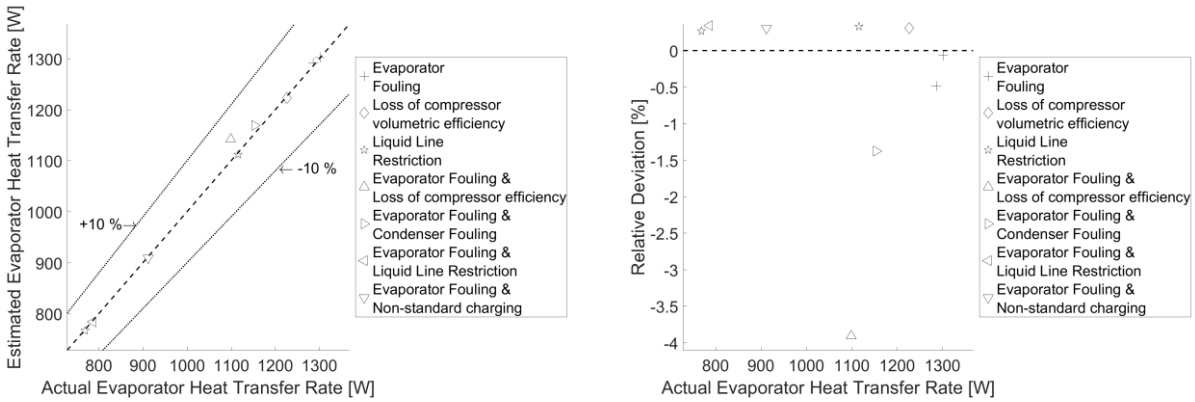

Figure 5: Parity plot (left) and residual plot (right) of evaporator validation set heat transfer rate actual vs. predicted values

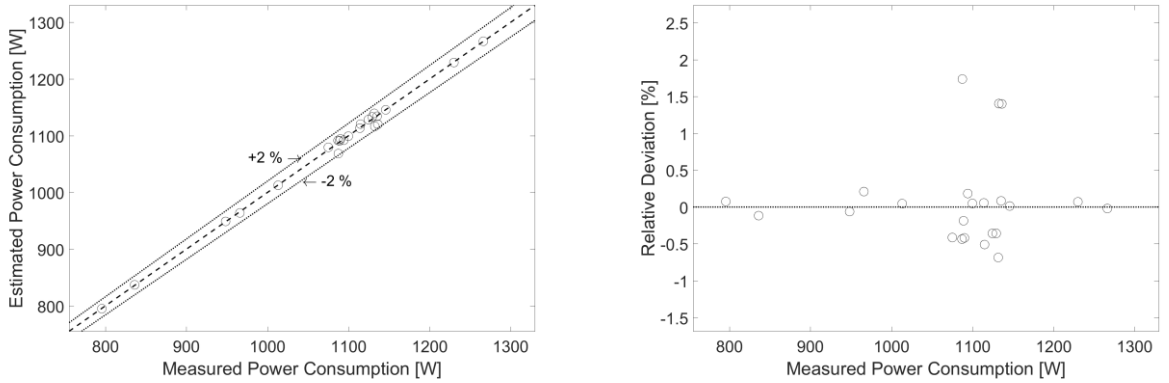

Figure 6: Parity plot (left) and residual plot (right) of compressor training set power consumption measured vs. predicted values

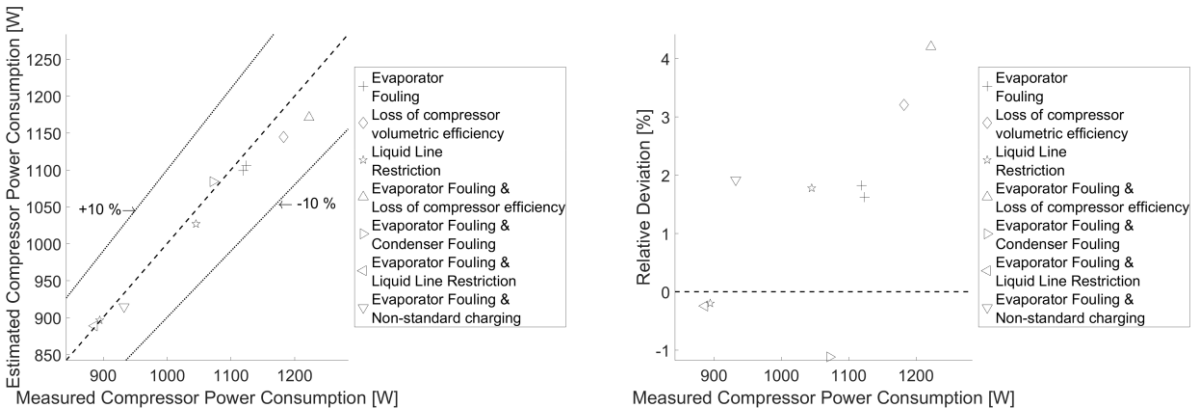

Figure 7: Parity plot (left) and residual plot (right) of compressor validation set power consumption measured vs. predicted values

Figures 6 and 7 show the training and validation results of the compressor power consumption model that shows good prediction performances.

4. CONCLUSION

This paper described the necessary steps and processes to create semi-empirical component models for major components of a commercial walk-in freezer with the use of a limited set of laboratory measurement data.
The literature review in this paper showed that there are sufficient existing semi-empirical or empirical component models to create a detailed and fault-enabled computer simulation of such systems. Numerical results showed that the existing semi-empirical models in the literature can successfully be applied to the major components of such systems, such as the compressor and heat exchangers, to predict important performance indices of a refrigeration system with good accuracy. To avoid extrapolative predictions with models that resemble a black-box model in terms of the number of coefficients, such as the 10-coefficient compressor models, an inclusive training dataset is preferred. Furthermore, the review of the receiver models in the literature showed that the volumetric data of the refrigeration system components are required for steady-state charge modeling in systems with a liquid line receiver. As future research, individual component models will be connected together to form a cycle model. A solver will be used to solve the cycle model implicitly with the use of a few input variables such as the ambient condition and fault levels.

5. NOMENCLATURE

Nomenclature	
A	Area
c	Specific heat
C	Regression coefficient
FDD	Fault detection and diagnostics
h	Enthalpy
HVAC&R	Heating ventilation and air conditioning and refrigeration
K	Conductivity
m	Mass flow rate
M	Absolute amount of mass
MPC	Model predictive control
n	Regression coefficient
NTU	Number of Transfer Units
P	Pressure
Q	Heat transfer
SC	Subcooling
T	Temperature
TXV	Thermostatic expansion valve
U	Thermal resistance
UA	Heat transfer conductance
V	Volume
var	Variable
W	Power
Y	Function output
Greek	
ε	Objective function output
ρ	Density
∅	Phase
μ	Kinematic viscosity
ω	Area ration

Subscripts	
a	Air
acc	Acceleration
amb	Ambient
b	Bulb
c	Condensing
comp	Compressor
cond	Condenser
cri	Critical
e	Evaporator
HL	Heat loss
i	Data point index
in	Inlet
l	Liquid
m	Number of coefficients
max	Maximum
n	Number of variables
out	Outlet
r	Refrigerant
rated	A normalization parameter
reg	Regression
sat	Saturated
tp	Two-phase
v	Vapor
z	Number of data points

6. REFERENCES

ASHRAE. (2015). Advanced energy design guide for grocery stores - Achieving 50% energy savings toward a net zero energy building. ASHRAE, Atlanta, Georgia.

Assawamartbunlue, K., and M. J. Brandemuehl. (2000). The Effect of Void Fraction Models and Heat Flux Assumption on Predicting Refrigerant Charge Level in Receivers. *International Refrigeration and Air Conditioning Conference* (489–496). Purdue University, West Lafayette, Indiana.

Assawamartbunlue, K., and M. J. Brandemuehl. (2006). Refrigerant leakage detection and diagnosis for a distributed refrigeration system. *HVAC&R Research* 12(3):389–405.

Behfar, A., D. P. Yuill, and Y. Yu. (2017). Automated fault detection and diagnosis methods for supermarket equipment (RP-1615). *Science and Technology for the Built Environment* 23(8):1253–1266.

Bell, I. (2010). ACHP 1.4 documentation. ACHP. http://achp.sourceforge.net/

Bergman, T. L., F. P. Incropera, D. P. DeWitt, and A. S. Lavine. (2011). *Fundamentals of heat and mass transfer*. Seventh edition. John Wiley & Sons., Hoboken, New Jersey.

Chen, W., and S. Deng. (2006). Development of a dynamic model for a DX VAV air conditioning system. *Energy Conversion and Management* 47(18):2900–2924.

Cheung, H. (2014). Inverse modeling of vapor compression equipment to enable simulation of fault impacts. Doctoral Dissertation in Mechanical Engineering. Purdue University, West Lafayette, Indiana.

Cheung, H., and J. E. Braun. (2013). Simulation of fault impacts for vapor compression systems by inverse modeling. Part I: Component modeling and validation. *HVAC&R Research* 19(7):892–906.

Dabiri, A. E., and C. K. Rice. (1981). A compressor simulation model with corrections for the level of suction gas superheat. *ASHRAE Transactions* 82(2):771–782.

Eames, I. W., A. Milazzo, and G. G. Maidment. (2014). Modelling thermostatic expansion valves. *International Journal of Refrigeration* 38:189–197.

Finlayson, S. M., and T. R. Dickson. (2004). R134a Liquid Level in a Receiver-Drier During Charge Determination, Steady State, and Transient Conditions. *SAE Technical Paper*. Detroit, Michigan.

Izadi-Zamanabadi, R., K. Vinther, H. Mojallali, H. Rasmussen, and J. Stoustrup. (2012). Evaporator unit as a benchmark for plug and play and fault tolerant control. *8th IFAC Symposium on Fault Detection* (701–706), August 29-31. Mexico City, Mexico.

Kim, W., and J. E. Braun. (2016). Development and evaluation of virtual refrigerant mass flow sensors for fault detection and diagnostics. *International Journal of Refrigeration* 63:184–198.

Li, H., and J. E. Braun. (2008). A method for modeling adjustable throat-area expansion valves using manufacturers' rating data. *HVAC&R Research* 14(4):581–595.

Llopis, R., R. Cabello, and E. Torrella. (2008). A dynamic model of a shell-and-tube condenser operating in a vapour compression refrigeration plant. *International Journal of Thermal Sciences* 47(7):926–934.

Oussar, Y., and G. Dreyfus. (2001). How to be a gray box: dynamic semi-physical modeling. *Neural Networks* 14(9):1161–1172.

Parker. (2016). Accumulators and Receivers. Catalog C-1, Parker, Machesney Park, Illinois.

Parrino, M., M. Dongiovanni, M. Milone, and M. Chiara. 1999. Influence of Receiver Capacity on the Refrigerant Charge and on the Performance of an A/C System. *SAE Technical Paper* (1–7). Detroit, Michigan.

Rajapaksha, L., and K. O. Suen. (2004). Influence of liquid receiver on the performance of reversible heat pumps using refrigerant mixtures. *International Journal of Refrigeration* 27(1):53–62.

Rasmussen, B. P., and A. G. Alleyne. (2006). Dynamic modeling and advanced control of air conditioning and refrigeration systems. University of Illinois at Urbana-Champaign, Report ACRC TR-244.

Schalbart, P., D. Leducq, and G. Alvarez. (2015). Ice-cream storage energy efficiency with model predictive control of a refrigeration system coupled to a PCM tank. *International Journal of Refrigeration* 52:140–150.

Standard AHRI. (2015). AHRI Standard 540 for Performance Rating of Positive Displacement Refrigerant Compressors and Compressor Units. Air-Conditioning, Heating, and Refrigeration Institute, Arlington, Virginia.

Strupp, N. C., J. Kohler, W. Tegethoff, N. Lemke, and R. Kossel. (2010). Energy efficient future automotive condenser systems. 2010 International Symposium on Next-Generation Air Conditioning and Refrigeration Technology (1–8), New Energy and Industrial Technology Development. Tokyo, Japan.

Techarungpaisan, P., S. Theerakulpisut, and S. Priprem. (2007). Modeling of a split type air conditioner with integrated water heater. *Energy Conversion and Management* 48(4):1222–1237.

Wei, D., X. Lu, and J. Gu. (2008). Dynamic modeling and simulation of an Organic Rankine Cycle (ORC) system for waste heat recovery. *Applied Thermal Engineering* 28(10):1216–1224.

Wichman, A., and J. Braun. (2009). Fault detection and diagnostics for commercial coolers and freezers. *HVAC&R Research* 15(1):77–99.

Wirz, D. (2009). Commercial Refrigeration: For Air Conditioning Technicians. Cengage Learning, Clifton Park, NY: Delmar.

Yin, X. H., and S. Y. Li. (2016). Model Predictive Control for Vapor Compression Cycle of Refrigeration Process. *International Journal of Automation and Computing*. 1–9. https://doi.org/10.1007/s11633-015-0942-6